INFORMATION-DEPENDENT LEAD-TIME MAPS FOR EARTHQUAKE EARLY WARNING IN THE CAMPANIA REGION

I. Iervolino [1], C. Galasso [2] and G. Manfredi [3]

[1] *Assistant Professor, Dipartimento di Ingegneria Strutturale, Università Napoli Federico II, Naples, Italy.*
[2] *PhD student, Dipartimento di Ingegneria Strutturale, Università Napoli Federico II, Naples, Italy.*
[3] *Professor, Dipartimento di Ingegneria Strutturale, Università Napoli Federico II, Naples, Italy.*
Email: iunio.iervolino@unina.it, carmine.galasso@unina.it, gaetano.manfredi@unina.it.

ABSTRACT :

Feasibility of earthquake early warning systems (EEWS) depends on the possibility of immediately detecting the earthquake's characteristics and on the ability to design applications for real-time seismic risk mitigation. Rapid estimation of event's features (as magnitude and location) is the focus of real-time seismology; the second issue requires particular attention of engineers. Among the information needed to design EEW engineering applications (and to evaluate the effectiveness of EEWS) there is the estimation of the available time to perform security actions before the arrival of the more energetic seismic phase at the site of interest; this interval is termed lead-time. The study presented herein examines the distributions of the available lead-time in the Campania (southern Italy) region. The study considers events occurring in the area covered by the ISNet (Irpinia Seismic Network) infrastructure and assumes a spatially-uniform distribution for the hypocenters. Under these hypotheses the minimum, maximum and average lead-times were computed. Also the uncertainties associated to the information provided by the ISNet are considered in order to evaluate the lead-time; in fact, there is a trade-off between the amount of warning time and the level of information available to predict the peak ground shaking. Results of the analyses, presented in form of maps, confirm that evacuation of building is hardly possible in the region, although the available warning time seems to be sufficient to activate personal and/or automated security measures.

KEYWORDS: Earthquake Early Warning, Real-time PSHA, lead-time.

1. INTRODUCTION

It is almost an achieved goal that, in the case of an earthquake, distributed seismic monitoring infrastructures can be used to effectively spread the alarm in advance to a broad audience via traditional media. For example, on 1st October 2007 the Japan Meteorological Agency (JMA) started providing residents in Japan with earthquake early warnings through media such as TV and radio. Other EEWS are currently under development or have been operational for experimental purposes in countries as Mexico, Taiwan, and Turkey. These systems are made of distributed seismic stations and use a variety of techniques to assess the real-time hazard associated with an earthquake and to deliver the warning information to end users. However, there is still a challenge for both engineers and seismologists to develop integrated systems able to effectively reduce the seismic risk in real-time in areas where the available warning time is low and the risk mitigation actions should be automated. This is the case, for example, of the Campania region (southern Italy).
Campania, being 13.595km² wide, is the twelfth largest region in Italy, but 5.8 million inhabitants make it the second most populous, and the most densely populated. At the same time, the most hazardous seismogenic source in the region is close, if not overlapped, to densely urbanized areas. In fact, high macro-seismic intensity earthquakes occurred over the centuries.
Campania was recently provided with an advanced regional seismic sensors network, also devoted to earthquake early warning purposes. The Irpinia Seismic Network (ISNet) is a modern infrastructure at the core of the ongoing EEWS, under development in southern Italy. The main targets of the network are: to monitor the activity of the area with a significant seismic potential, to provide real-time alerts to selected targets for

moderate-to-large earthquakes, and to measure/estimate in near-real-time (in the immediate post-event) ground shaking in the region.

ISNet is a local network of strong motion, short period and broad band seismic stations deployed in a 100 x 70km^2 area along the southern Apenninic chain, covering the epicentral area of the main earthquakes that occurred in the region, including the magnitude 6.9, 23th November 1980, event. The seismic network is composed of 29, 6-components stations equipped with both accelerometers and velocimeters (and with real-time telemetry) organized in six sub-nets, each of them composed of a maximum of 6-7 stations. The stations of each sub-net are connected in real-time to a central data-collector named Local Control Center (LCC). The different LCCs are linked among them and to a Network Control Center (NCC), located at RISSC (http://www.rissclab.unina.it), 100km away from the network center. The ISNet is conceived as a system where the levels of computation, analysis and decision are distributed over the seismic network nodes. Each node of the network should be able to process and analyze in real-time the first P-wave signal, providing the measured quantities (arrival time, frequency, amplitude) to its closest LCC. As more stations will record the seismic signal, the new measurements may be sent to and processed by the LCC, which crosschecks the redundant information coming from different stations, and outputs a progressively refined estimate of earthquake location and magnitude (Weber et al., 2007). Alternatively, the NCC may process the information and provide estimates on the earthquake's characteristics.

The EEWS under development in Campania using ISNet has been designed to be a hybrid application of regional and on-site early warning approaches (Kanamori, 2005). In fact, there is a potential for a regional seismic infrastructure to operate as an EEWS and to protect several critical targets at the same time. Such EEWS's may prove to be a moderately costly solution for the reduction of the expected earthquake losses in large regions. The exploitation of regional seismic networks for the protection of multiple critical systems depends: (i) on the possibility of real-time estimation of the size of the event (source parameters) or (most importantly) the intensity of subsequent ground shaking at various sites and; (ii) on the ability to design engineering applications for real-time seismic risk mitigation. Among the information needed to design earthquake early warning applications, there is the estimation of the available time to perform security actions before the arrival of the more energetic seismic phase at the site of interest, this interval is termed lead-time. Herein, the available lead-time is computed for the Campania region in a probabilistic manner.

Because, in the developed approach to EEW (summarized in the following), the information on the ground motion evolves as the number of seismic stations triggered by the event increases, there is a trade-off between the available time and the level of information for the estimation of the earthquake potential. Therefore, the study presented investigates on the required number of triggered stations to stabilize the real-time prediction of peak ground shaking and how it is affected by different sources of uncertainty. Finally, different lead-time maps are computed as a function of the level of information available (i.e., the number of stations triggered) and selected results are analyzed in respect to potentially operable security actions.

2. REAL-TIME RISK ANALYSIS FOR EARTHQUAKE EARLY WARNING

Seismologists have recently developed several methods to estimate the event's magnitude (*M*) on the basis of limited information of the P-waves (in the first few seconds of the recorded ground motion) for real-time applications. Similarly, the source-to-site distance, *R*, may be predicted analyzing the order in which the seismic stations detect the developing earthquake. Therefore, it is possible to assume that at a given instant estimates of *M* and *R* are available, and the prediction of ground motion at the site can be performed as the probabilistic seismic hazard analysis (PSHA) conditional to the real-time information given by the seismic sensors network (Iervolino et al., 2006). In fact, let's assume that a given time *t* from the earthquake's origin, the seismic network can provide estimates (in terms of probability density functions or PDFs) of *M* and *R*. The PDF of *M* is intrinsically conditioned to a vector of measures of the seismic instruments useful to predict the magnitude, say $\{\tau_1, \tau_2,..., \tau_n\}$, where *n* is the number of instruments at which data are available. The PDF of *M* has to be indicated as $f_{M|\tau_1,\tau_2,...,\tau_n}(m|\tau_1,\tau_2,...,\tau_n)$. Similarly, the PDF of *R*, which according to the considered localization method (Satriano et al., 2008) only depends on the sequence of stations triggered, will be referred to as $f_{R|s_1,s_2,...,s_n}(r|s_1,s_2,...,s_n)$, where $\{s_1, s_2,..., s_n\}$ is such sequence. Thus, it is possible to compute the

probabilistic distribution (or hazard curve) of a ground motion intensity measure (*IM*) at the site (i.e., the peak ground acceleration or PGA) as in Eqn. 1.1. This also requires an attenuation relationship, $f_{IM|M,R}(im|m,r)$, available for the chosen *IM*. The subscript *n* in the left-hand side of Eqn. 1.1 means that the computed hazard curve refers to a particular set of triggered stations (at time in which the integral is computed) and, therefore, evolves with time until all stations have measured the data of interest.

$$f_{IM,n}(im) = \iint_{m\ r} f_{IM|M,R}(im|m,r)\ f_{M|\tau_1,\tau_2,...,\tau_n}(m|\tau_1,\tau_2,...,\tau_n)\ f_{R|s_1,s_2,...,s_n}(r|s_1,s_2,...,s_n)\ dr\ dm \qquad (1.1)$$

The real-time hazard integral requires the distribution of magnitude estimated on the basis of data provided by the network at given time. For example, Allen and Kanamori (2003) developed a relationship between the magnitude of the event and the predominant period, τ, of the first four seconds of the velocity recording of the P-waves. Zollo et al. (2006) show that the low-pass filtered, peak amplitudes of initial P- and S-wave seismic signals recorded close to an occurring earthquake source correlate with the magnitude.
It has been shown (Iervolino et. al, 2006; Iervolino et al., 2007) that if the distribution of any of this parameter is available conditional to magnitude, $f_{\tau|M}(\tau|m)$, then evolutionary $f_{M|\tau_1,\tau_2,...,\tau_n}(m|\tau_1,\tau_2,...,\tau_n)$ may be easily computed in a Bayesian updating approach in which the *prior* distribution is given by the Gutenberg-Richter relationship for the source. On the other hand, also $f_{R|s_1,s_2,...,s_n}(r|s_1,s_2,...,s_n)$ may be available because of rapid earthquake localization procedures. One of the most recent is that based on the Equal Differential-Time (EDT) formulation (Satriano et al., 2008). The algorithm defines a dense (1km spaced) grid of points, each of those identified by a set of coordinates in the space below the network. During an earthquake the algorithm allows to assign to each point a probability that hypocenter is coincident with that point. Consequently, the estimate of the epicentral distance may be retrieved by a geometrical transformation assigning, to any particular distance value, a probability which is the sum of the probabilities of all points of the grid with the same distance to the site.

2.1. A virtual simulator as a tool for testing the performance of the ISNet Early Warning Infrastructure

To analyze the performances of the ISNet early warning infrastructure in the case of moderate-to-large magnitude earthquakes a MATLAB-SIMULINK® simulator was developed. It allows to represent the behavior of the ISNet-EEWS without recorded signals, although this implies some intrinsic limitations. The flow chart of the simulator may be represented by three main bocks: acquisition, computation, and alarm issuance decision.
Acquisition. Simulation starts with the assignment of the geophysical features the EEWS will try to estimate (*true* values of magnitude and location). Once the event is defined (by *M* and source-to-site distance *R*), the measurements of τ for the triggered stations are needed to perform the real-time risk analysis. It is possible to simulate the station measurements by sampling the empirical distribution of τ conditional on the true magnitude of the event. In the simulation process, at any given time *t*, the number and sequence of stations triggered is computed assuming an appropriate velocity model for the region (to follow). A measurement of a station is considered in the process if 4s have passed from its trigger. Then, the measurement vector $\{\tau_1,\ \tau_2,...,\ \tau_n\}$ is broadcasted from the acquisition block to the computation block.
Computation. This block collects data, and starts to furnish an evolving estimation of the hypocenter (i.e., the distance of the source from a site of interest) and the magnitude of the earthquake with the associated PDFs. The magnitude is estimated using the empirical relationship with τ measured in the first 4s of the record in a Bayesian approach. The location algorithm, RTLoc (Satriano et al., 2008) covers the area of interest with Voronoi cells and back-propagates the travel-times given the velocity model: the epicenter location is generally stable when 3 or 4 stations have triggered the event. At each time step, the PDFs of *R* and *M* are updated integrating the new information.
Decision. Whether to issue or not an alarm, during a running earthquake, depends on a decisional rule. Such a rule is based on the probability of exceeding a given threshold (IM_c) for a certain ground motion *IM*. Starting from the *R* and *M* PDFs, the IM distribution at the target site is computed through the hazard integral. Assuming that the predicted IM is the PGA, the alarm is issued if the condition of Eqn. 2.1 occurs. In other words, the

alarm is issued when the risk that the critical peak ground motion value is exceeded, is larger than a probability threshold P_c.

$$P[PGA > PGA_c] > P_c \tag{2.1}$$

2.1.1. Numerical tests and uncertainty analysis

As an example, results of simulation for an *M* 6 event located within the network are given. The target sites, used for the simulation, are Naples and S. Angelo dei Lombardi (Avellino), a town destroyed by 1980 Irpinia earthquake. The epicenter of the simulated event is 124km far from Naples and 60km far from S. Angelo dei Lombardi (Figure 1, left). The probabilistic estimations of the magnitude Figure 1 (right) and source-to-site distance (epicentral) are given in Figure 2 in terms of PDFs. In Figure 3 the real-time hazard is given in terms of PGA for the considered sites (the used attenuation relationship is from Sabetta and Pugliese, 1996). Curves in Figures 1-3, correspond different numbers of triggered stations during the developing seismic event, i.e., are function of time. Note that the hazard increases as time flows (more τ measures are available because more stations are triggered), consistently with the magnitude estimation method, which tends to underestimate *M*, especially at the beginning of the event (Iervolino et al., 2006).
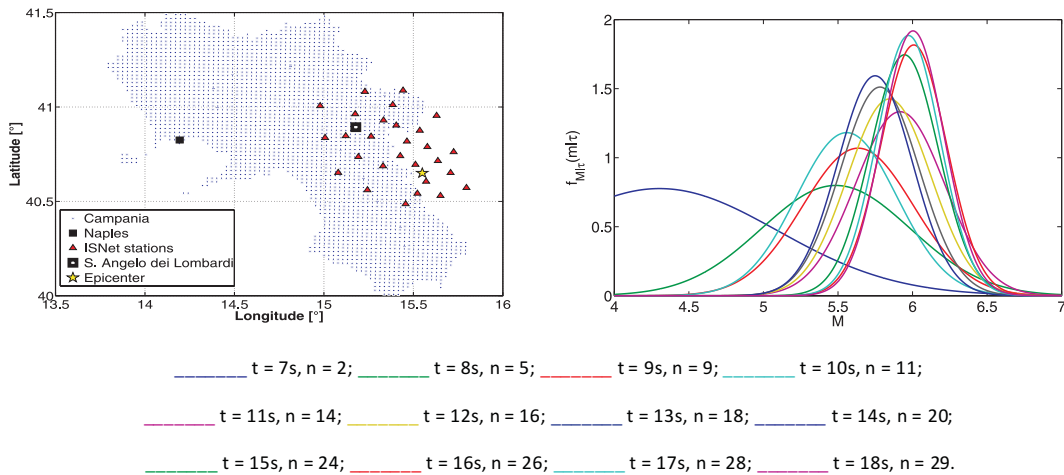

_____ t = 7s, n = 2; _____ t = 8s, n = 5; _____ t = 9s, n = 9; _____ t = 10s, n = 11;

_____ t = 11s, n = 14; _____ t = 12s, n = 16; _____ t = 13s, n = 18; _____ t = 14s, n = 20;

_____ t = 15s, n = 24; _____ t = 16s, n = 26; _____ t = 17s, n = 28; _____ t = 18s, n = 29.

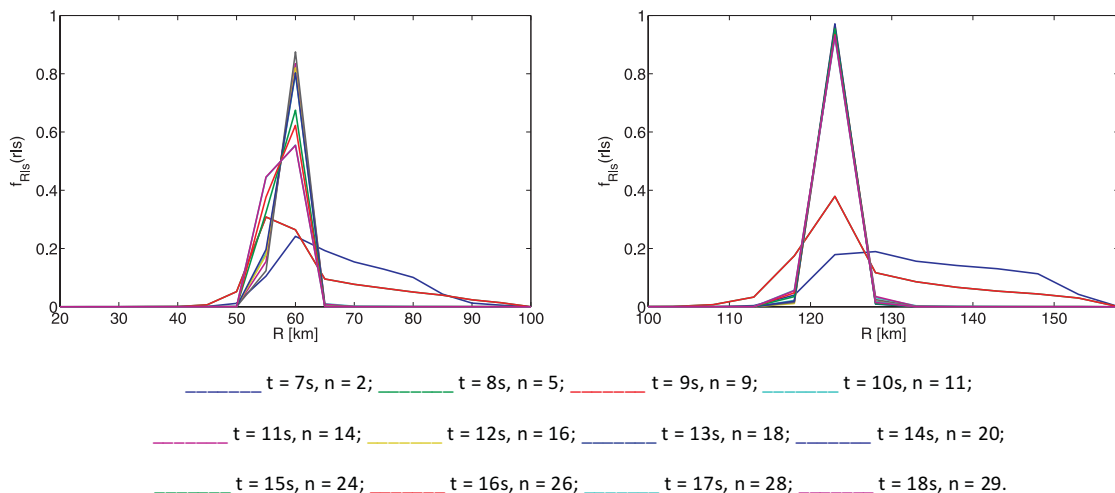Figure 1. Location of the event and sites (left); PDFs of *M* as the number of triggered stations increases (right).

_____ t = 7s, n = 2; _____ t = 8s, n = 5; _____ t = 9s, n = 9; _____ t = 10s, n = 11;

_____ t = 11s, n = 14; _____ t = 12s, n = 16; _____ t = 13s, n = 18; _____ t = 14s, n = 20;

_____ t = 15s, n = 24; _____ t = 16s, n = 26; _____ t = 17s, n = 28; _____ t = 18s, n = 29.

Figure 2. PDFs of *R* as the number of triggered stations increases for S. Ang. dei Lomb. (left) and Naples (right).

_____ t = 7s, n = 2; _____ t = 8s, n = 5; _____ t = 9s, n = 9; _____ t = 10s, n = 11;

_____ t = 11s, n = 14; _____ t = 12s, n = 16; _____ t = 13s, n = 18; _____ t = 14s, n = 20;

_____ t = 15s, n = 24; _____ t = 16s, n = 26; _____ t = 17s, n = 28; _____ t = 18s, n = 29.
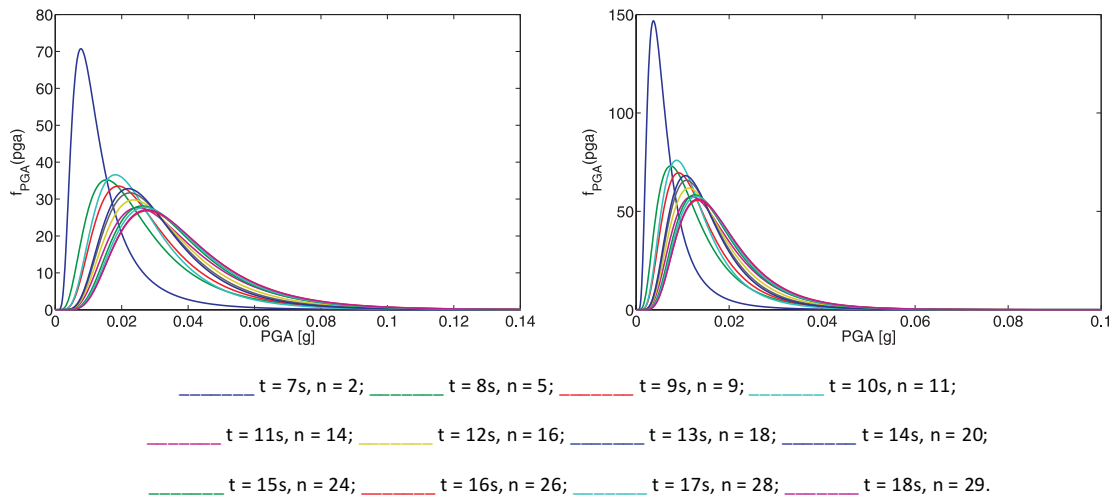
Figure 3. PDFs of PGA as the number of triggered stations increases for S. Ang. dei Lomb. (left) and Naples (right).

In Figure 4 the exceedance probabilities are given for different possible values of the critical PGA_c of the decisional rule of Eqn. 2.1. The plots in the figure refer to 100 simulations of the same event discussed above, which means that the τ measures have been simulated 100 times for the same M 6 earthquake. It appears that the exceedance probability of the critical PGA does not change after 10s-13s, which corresponds, on average, to 11-18 stations measuring τ.

In Figure 5, the coefficient of variation (CoV, the ratio of the standard deviation to the mean) of the PGA is given for different conditions, as the number of triggered stations increases. In particular, the CoV of the PGA is computed, via the integral of Eqn. 1.1, in the following cases: (i) considering both PDFs of M and R; (ii) considering only the mode of R without its full PDF; and (iii) considering only the mode of R and the mean of M (Convertito et al., 2008). This allows to assess the effects of uncertainty in estimation of M and R on the distribution of the PGA.

It appears from the results that uncertainty on distance is negligible in respect to the prediction of PGA (CoV of PGA does not vary significantly considering or not uncertainty on distance); also uncertainty on magnitude, although larger than distance, is small if compared to that of the attenuation law, at least when several measures of τ are available.
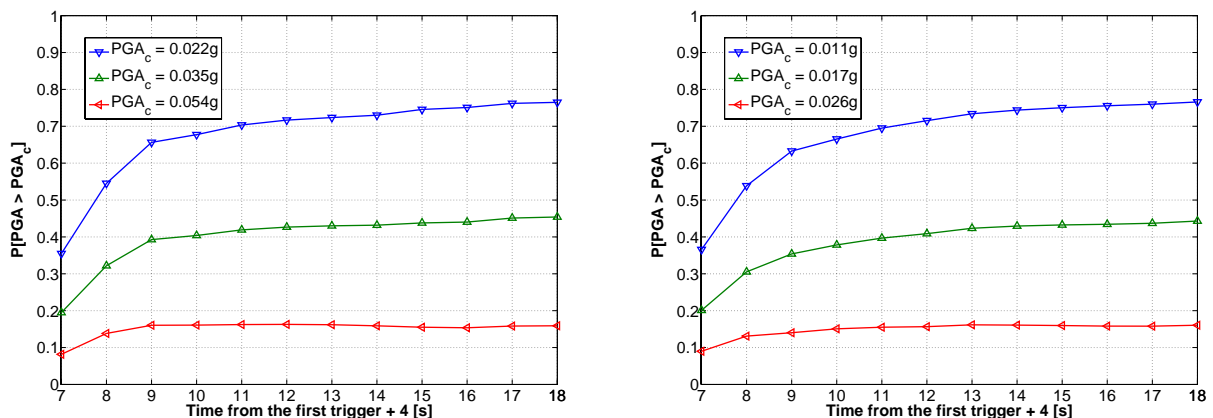

Figure 4. Estimation of exceedance probability for some PGA values as the number of triggered stations increases, for S. Ang. dei Lomb. (left) and Napoli (right), for 100 simulated events.
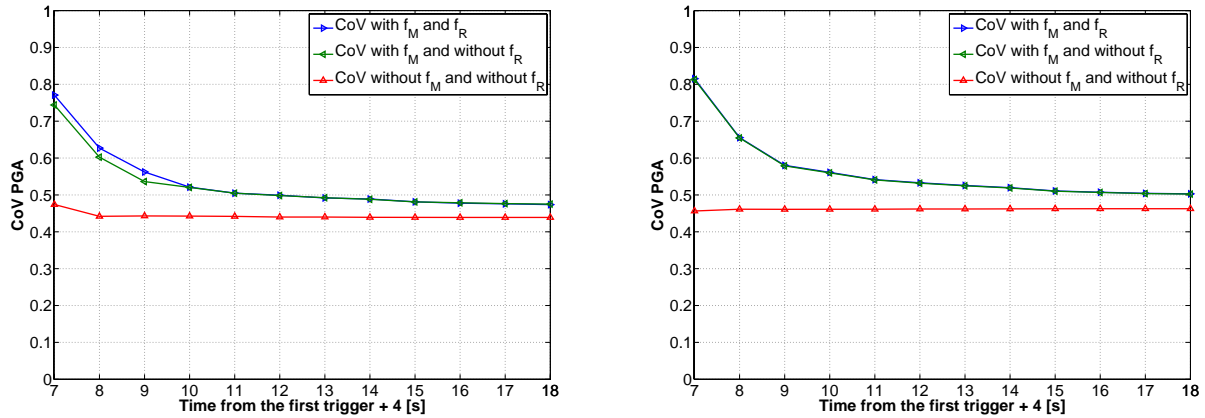
Figure 5. CoV of PGA computed considering the full PDFs of M and R or their point estimates, for S. Ang. dei Lomb. (left) and Napoli (right), for 100 simulated events.

3. INFORMATION-DEPENDENT LEAD-TIME

EEW is based on the difference in speed between mechanic and radio signals and on the fact that the most of the seismic energy is brought by S-waves, while information on the earthquake size and location can be taken from P-waves which are faster. Thus, if computing is fast enough, it is possible to use part of the time before S-wave arrival at the site of interest to perform rapid evaluation of earthquake parameters, the remaining time is to issue the alarm and undertake security actions; it is termed lead-time.

It has been shown that, in the adopted approach, the estimation of critical ground motion becomes stable only after a number of stations have recorded the early signal of the event, therefore, there is a trade-off between the lead-time and the level of information for the alarm issuance. In fact, different definitions of lead-time are considered in the following, each of those correspond to a different number of stations triggered (i.e., a different level of information on magnitude and location of the event). For each of these proposed definitions, the minimum, maximum and average lead-times associated to each point (*j*) in Campania, have been computed using an appropriate regional 1D velocity model. According to this model P and S velocities, v_P and v_S respectively, are function of hypocentral depth and have a constant of 1.68 ratio (Satriano et al., 2008). In this framework the lead-time, T_k^j, for each point may be computed as:

$$T_k^j = T_S^j(h) - T_P^k(h) - \Delta t \tag{3.1}$$

where, $T_S^j(h)$ is the S-wave arrival time at observation point (*j*) and depends on the source depth h; $T_P^k(h)$ represent the time to trigger the first *k* stations and also depends on the source depth h because of the velocity model; Δt is the required processing time (assumed equal to 5 seconds and includes the required P-wave data recording at each station). $T_S^j(h)$ and $T_P^k(h)$ can be approximated using travel-time curves as a function of distance from the seismic source and h (A. Zollo, personal communication, 2008).

Lead-time has been computed for k = 4, k = 18 and k = 29 considering as possible epicenters those occurring in the rectangular area which includes the ISNet sensors (to account for events occurring within the network), while the hypocentral depth may be up to 12km. Within this bounds the hypocentral location has been extracted randomly. Given the geometry of the ISNet infrastructure and the velocity model above, the elapsed time for 1 station to detect the P-wave arrival is on average 1.5s and ranges from 1s to 4s for all events of the type considered; for 18 stations is, on average, 7.5s ranging from 5s to 11s; finally, the average time to trigger all 29 ISNet stations is 12s ranging from 8s to 16s. Results in form of maps are given in Figure 6, where minimum, average, and maximum lead-time are given for each node of a regular grid having about 2km spacing and covering the Campanian territory with over 2700 nodes. In the figure the "blind zones", areas in which no warning time is available, are also given. Maps can be analyzed in respect to a list of real-time risk reduction actions and the time they require (Goltz, 2002); an example is given in Figure 7.
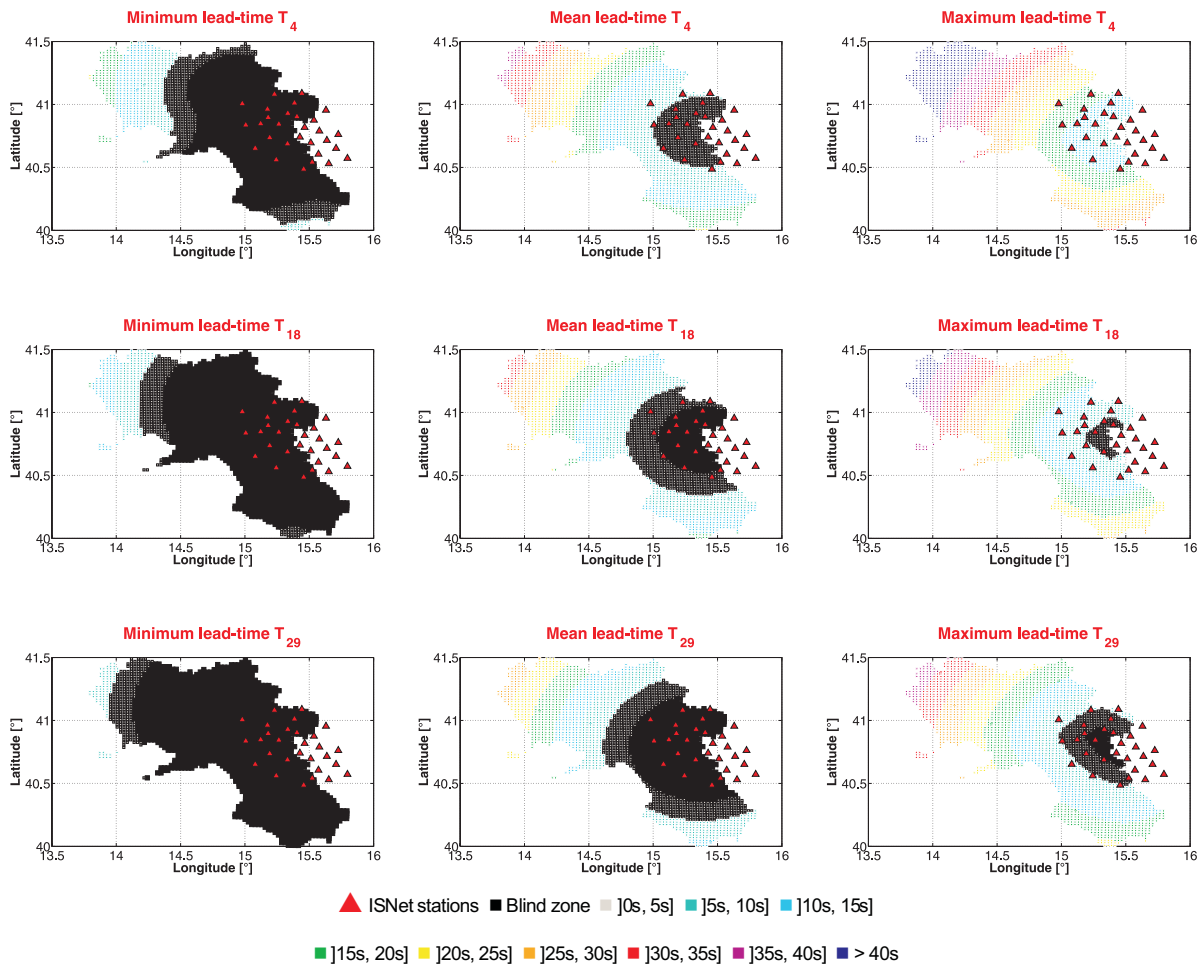
Figure 6. Lead-time maps for different numbers of stations triggered.
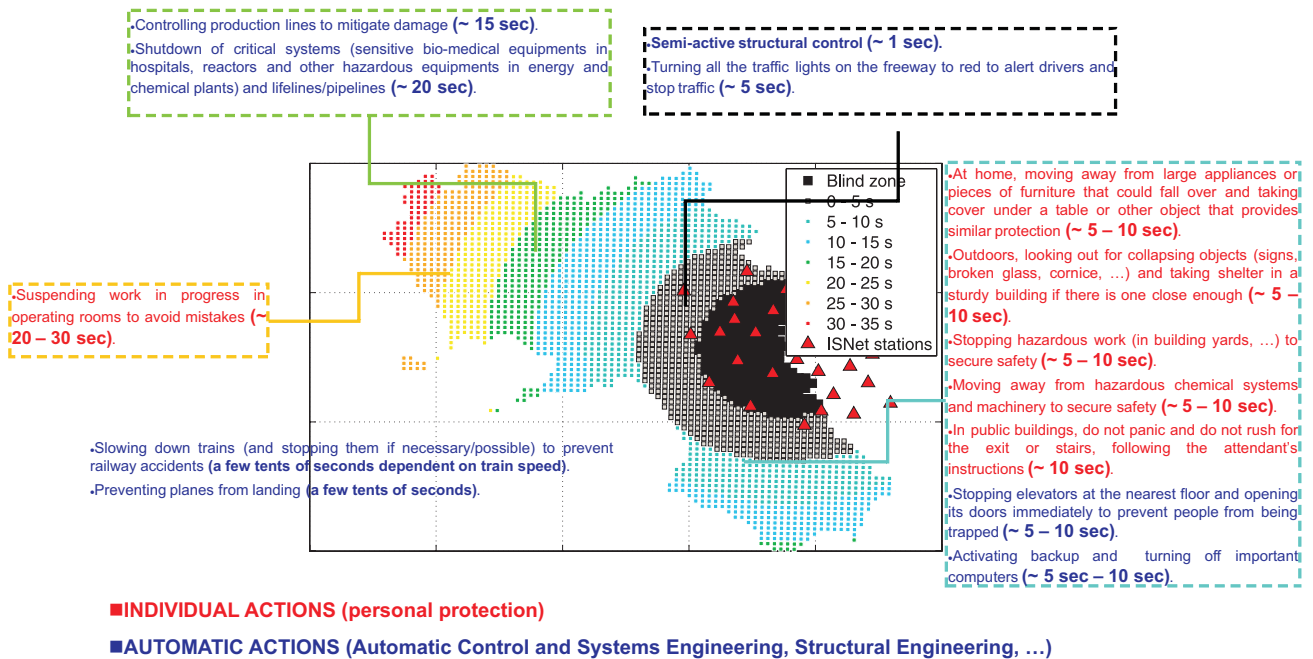

Figure 7. Average lead-time with the information of 18 stations and security actions, adapted from Goltz (2002).

4. CONCLUSIONS

The study presented investigated the trade-off between the information on the incoming earthquake and available lead-time for earthquake early warning purposes. The study was carried out for the Campania (southern Italy) which is provided with a regional seismic network, ISNet, with real-time features.

Results of the uncertainty analyses suggest that: (1) the larger uncertainty in the prediction of peak ground motion at the site is that of the attenuation relationship; and (2) that, according to the magnitude estimation approach considered, several stations have to record the early seconds of the P-waves to stabilize the estimated risk of exceeding a critical PGA value.

Information-dependent lead-time maps confirm that evacuation of buildings is hardly possible in the region. However, the estimated warning times seem to be sufficient to activate several types of security measures in selected structures/infrastructures. In fact, EEWS could provide warning to at least some of the affected population in a damaging earthquake. These maps, which also provide the size of the blind zone, can be also used as a guide to select strategic locations for future network development.

AKNOWLEDGEMENTS

REFERENCES

Allen, R.M., and Kanamori, H. (2003). The Potential for Earthquake Early Warning in Southern California, *Science*, **300** 786–789.

Convertito, V., Iervolino, I., Giorgio, M., Manfredi, G., and Zollo, A. (2008) Prediction of response spectra via real-time earthquake measurements, *Soil Dynamics and Earthquake Engineering*, **28**, 492–505.

Goltz, J.D. (2002). *Introducing Earthquake Early Warning in California: A Summary of Social Science and Public Policy Issues*, A Report to OES and the Operational Areas, California Governor's office for Emergency Services. [http://www.cisn.org/docs/Goltz.TaskI-IV.Report.doc]

Kanamori, H. (2005). Real-time seismology and earthquake damage mitigation, *Annual Review of Earth and Planetary Science,* **33**, 195–214.

Iervolino, I., Convertito, V., Giorgio, M., Manfredi, G., and Zollo, A. (2006) Real-time risk analysis for hybrid earthquake early warning systems, *Journal of Earthquake Engineering*, **10**, 867–885.

Iervolino, I., Giorgio, M., and Manfredi, G. (2007). Expected loss-based alarm threshold set for earthquake early warning systems, *Earthquake Engineering and Structural Dynamics*, **36**, 1151–1168.

Satriano, C., Lomax, A., and Zollo, A. (2008). Real-Time Evolutionary Earthquake Location for Seismic Early Warning, *Bulletin of the Seismological Society of America,* **98**, 1482–1494.

Sabetta, F., and Pugliese, A. (1996). Estimation of response spectra and simulation of nonstationarity earthquake ground motion, *Bulletin of the Seismological Society of America*, **86**, 337–352.

Weber, E., Convertito, V., Iannaccone, G., Zollo, A., Bobbio, A., Cantore, L., Corciulo, M., Di Crosta, M., Elia, L., Martino, C., Romeo, A., and Satriano, C. (2007). An Advanced Seismic Network in the Southern Apennines (Italy) for Seismicity Investigations and Experimentation with Earthquake Early Warning, *Seismological Research Letters*, **78**, 622–634.

Zollo, A., Lancieri, M., and Nielsen, S. (2006). Earthquake magnitude estimation from peak amplitudes of very early seismic signals on strong motion records, *Geophysical Research Letters*, **33**, L23312.